



Contents lists available at UGC-CARE

# International Journal of Pharmaceutical Sciences and Drug Research

[ISSN: 0975-248X; CODEN (USA): IJPSPP]

journal home page : <https://ijpsdronline.com/index.php/journal>

## Research article

# Phytochemical Screening, Isolation and Estimation of Bioactive lupeol, *In-vitro* and *In-silico* Neuroprotective Effect of Phytoconstituents from Karnasphota: *Cardiospermum halicacabum* Linn. Roots

Hiral R Topiya\*, Devang J Pandya

School of Pharmacy, RK University, Rajkot, Gujarat, India.

## ARTICLE INFO

### Article history:

Received: 09 July, 2024

Revised: 12 August, 2024

Accepted: 16 August, 2024

Published: 30 September, 2024

### Keywords:

Karnasphota, Phytochemicals, Lupeol, Neuroprotective, Ayurveda.

### DOI:

10.25004/IJPSDR.2024.160507

## ABSTRACT

The importance of herbals in neurodegenerative disorders lies in their ability to offer multifaceted therapeutic benefits, including neuroprotection, anti-inflammation, antioxidant effects and cognitive enhancement. Karnasphota is a memory enhancer as per Ayurveda and is described as Medhya. This claim is evaluated scientifically for the scope of treating neurodegenerative disorders. Proximate analysis and phytochemical profiling were performed after solvent extraction of the powdered root of *Cardiospermum halicacabum* L. An *in-vitro* DPPH antioxidant assay, acetylcholinesterase and tyrosinase enzyme inhibition effect were carried out to identify the capability of root extract as a neuro-shielding agent. The total content of bioactive triterpenoid lupeol was estimated by HPTLC, followed by its isolation. The total lupeol content as a bioactive marker found was 6.400 µg. The plant root phytoconstituents are potent antioxidants with IC<sub>50</sub> 89.08 µg, comparable to the positive control. The potency of the phytoconstituents was demonstrated by *in-vitro* inhibition of acetylcholinesterase and tyrosinase enzymes as compared to physostigmine and pregabalin, respectively, by HPLC that shows optimum potency compared to standards. An *in-silico* study against AChE evaluated the potential of the identified phytoconstituents. An *in-silico* study revealed most phytoconstituents are promising anti-Alzheimer's leads compared to donepezil, an acetylcholinesterase inhibitor.

## INTRODUCTION

AD is linked to brain cholinergic neurotransmission impairment and memory and focus decline.<sup>[1]</sup> Parkinson's disease (PD), a severe neurodegenerative disorder, causes the ventral midbrain's substantia nigra pars compacta to lose dopaminergic neurons, causing parkinsonism.<sup>[2,3]</sup> Both of these disorders impact older individuals, disrupting their daily activities. These disorders cannot be reversed, but we can only halt their further progression with the use of existing modern medicines. The herbal medicines mentioned in Ayurveda can be scientifically evaluated to discover alternative therapies for Alzheimer's

disease (AD), Parkinson's disease (PD), and related neurodegenerative disorders.<sup>[4,5]</sup>

Karnasphota, *Cardiospermum halicacabum* L., a Sapindaceae plant, is found throughout the tropic and subtropic regions of Asia and Africa. India has used it for centuries as Ayurvedic traditional medicine.<sup>[6,7]</sup> This plant is reported with numerous pharmacological properties, including antimicrobial, antioxidant, analgesic, vaso-depressant, and anti-inflammatory properties on the leaves and stems of the plant. The leaf extract with methanol from *C. halicacabum* Linn. demonstrated neuroprotective properties against scopolamine-induced neurotoxicity in

\*Corresponding Author: Ms. Hiral R. Topiya

Address: School of Pharmacy, RK University, Rajkot, Gujarat, India.

Email ✉: [topiyahiral@gmail.com](mailto:topiyahiral@gmail.com)

Tel.: +91-9106855805

**Relevant conflicts of interest/financial disclosures:** The authors declare that the research was conducted in the absence of any commercial or financial relationships that could be construed as a potential conflict of interest.

© The Author(s) 2024. **Open Access.** This article is licensed under a Creative Commons Attribution 4.0 International License, which permits use, sharing, adaptation, distribution and reproduction in any medium or format, as long as you give appropriate credit to the original author(s) and the source, provide a link to the Creative Commons licence, and indicate if changes were made. The images or other third party material in this article are included in the article's Creative Commons licence, unless indicated otherwise in a credit line to the material. If material is not included in the article's Creative Commons licence and your intended use is not permitted by statutory regulation or exceeds the permitted use, you will need to obtain permission directly from the copyright holder. To view a copy of this licence, visit <https://creativecommons.org/licenses/by/4.0/>

albino mice. It effectively modulated acetylcholinesterase activity throughout the brain, reduced amnesia caused by scopolamine, and improved learning and memory. The prior research on *Karnasphota* investigated the potential inhibitory effects of tyrosinase, acetylcholinesterase, and butyrylcholinesterase (AChE), as well as its potent antioxidant activities with the phytoconstituents of extracts obtained from seeds and aerial parts. The main chemical components identified through phytochemical analysis of seeds and above-ground parts were apigenin, apigenin-7-O-glucoside, and luteolin. Another study also demonstrated that the *C. halicacabum* Linn's alcoholic root extract exhibits potent anticonvulsant effects and minimal motor toxicity by enhancing GABAergic activity.<sup>[8,9]</sup> Prior research on *Karnasphota* indicated that the roots of the plant have strong anxiety-reducing properties. It has been discovered that cardiospermin, a cyanogenetic glucoside, is the specific compound extracted from the plant's root extract that possesses powerful anti-anxiety effects.<sup>[10,11]</sup> Ayurveda describes the roots and seeds of the *Karnasphota* as "Medhya" a memory enhancer, suggesting roots and seeds can be investigated in AD-related dementia and other neurodegenerative disorders like PD. The current study investigated the neuroprotective properties of *Karnasphota* root, as described in Ayurveda and investigated the specific bioactive phytoconstituents responsible neuroprotective effect.

## MATERIAL AND METHODS

### Procurement and Authentication of *C. halicacabum* L.

The seeds of the plant were obtained from Swathi natural herbs, Dindigul, Tamil Nadu. The seeds were then cultivated on the farm at the end of February 2022 and the seedlings were procured in May 2022. The plant was identified and verified at the Botany Department at Saurashtra University, Rajkot, Gujarat, and a specimen of the plant was deposited at Saurashtra University, Rajkot, and assessed for Quality parameters as per WHO Guidelines.<sup>[12,13]</sup>

### Successive Solvent Extraction of Roots

Air-dried roots of *C. halicacabum* Linn. were ground into a powder and put through a #10 sieve. All dried powders were precisely weighed 200 g on a digital scale before being put through a series of extractions using the soxhlet equipment for 7 hours separately using 500 mL solvents with descending polarities in order of petroleum ether, toluene, and methanol. The aqueous extract was prepared by reflux condensation for 6 hours. All of the extracts were concentrated and dried in a water bath.

### Phytochemical Screening of Methanolic Root Extract with HPLC

For phytochemical screening, HPLC is used. To check extract purity and for anti-Alzheimer's and anti-

Parkinson's activity, 1-mg of extracted sample was dissolved in the AR grade methanol and run in HPLC.<sup>[14]</sup>

### Acetylcholinesterase and Tyrosinase Inhibition Activity with Root Extract

The study investigated the inhibitory activity of acetylcholinesterase and tyrosinase by referring to various review literature. In this study, an extract with a 0.1 mg/mL concentration was combined with the enzymes AchE and tyrosinase at 1-mg/mL concentration each. Using the sonication technique, the absorbance was taken at a particular wavelength of 360 nm while the reaction was being carried out. The technique employed a binary gradient with mobile phases consisting of Methanol: Acetic acid (0.1%)[7:3 v/v] at a wavelength of 360 nm. In the control group, no extract was added. Based on the difference in the peak height of the enzyme and extract in the HPLC chromatogram, the potency of the root extract against tyrosinase and acetylcholinesterase was determined by comparing it with the same concentration of standard physostigmine and pregabalin.<sup>[14]</sup>

### Isolation of Bioactive Lupeol

A tiny quantity of acetone was used to dissolve the air-dried methanol extract before it was adsorbed with silica (60–120 mesh) and dried into a free-flowing powder. Then, using silica (60–120 mesh) as the stationary phase, it was subjected to column chromatography. Initially, 100% ethyl acetate was used as the eluting agent for the initial elution, and then 5, 10, 15, 20, 25, 50 and 75% ethyl acetate in toluene was used to increase the polarity. To further increase the polarity, 1, 5, 10, 25 and 50% methanol were added to the ethyl acetate. At each stage of fractionation, various fractions were gathered up to a 5 mL amount.<sup>[15]</sup> The fractions were examined using TLC with a mobile phase containing Toluene: Ethyl acetate: Formic acid (80: 15: 5). The fractions were detected at wavelengths of 254 and 366 nm using ultraviolet light. The identification of compounds in the fractions was verified by subjecting the developed plates to treatment with antimony trichloride and heated at 110°C temperature for 10 minutes. Preparative TLC purified the total four identified fractions containing marker for final separation of the chemical marker Lupeol.<sup>[15,16]</sup>

### Identification of Lupeol

The isolated lupeol was examined using different spectroscopic methods, including ultraviolet spectroscopy.

### Screening of Isolated Lupeol by TLC and HPTLC

#### TLC

The determination of thin-layer chromatography (TLC) was conducted on the methanolic root extract and isolated chemical marker.

Glass capillaries at the pencil-marked baseline were taken to apply the sample to the TLC plate. The chromatography



plate was then dried in the fume hood after the sample was added again and again until a dark spot appeared. The chamber was then filled with a solution of 20 mL of the mobile phase with toluene, ethyl acetate, and formic acid (10:8:2). The plate was placed in the liner of the upper chamber. After the experiment, the areas were marked on plates dried in the fume hood.<sup>[15,16]</sup>

#### Detection of the Spot

After every plate was dried, spots were detected using UV light with a wavelength of 254 nm. The retention factor (Rf) revealed a dynamic chemical flow.<sup>[16]</sup>

$$Rf = \frac{\text{Distance travelled by solute}}{\text{Distance travelled by the solvent front}}$$

#### HPTLC analysis

By contrasting it with crude methanolic extract, isolated lupeol from the methanol root extract of *C. halicacabum* was screened using HPTLC.<sup>[16]</sup>

#### Estimation of Bioactive Lupeol in Root Extract

The methanol extract of *C. halicacabum* root was used for the HPTLC analysis of lupeol. The extract was compared to standard lupeol solutions as part of the analysis. To make a stock solution of lupeol (0.1 mg/mL), precisely weighed 1-mg of standard pure lupeol was dissolved in 10 mL of ethanol. By further diluting the stock solution with solvent methanol, a standard solution of lupeol (100 µg/mL) was produced. This was the working concentration for the HPTLC method.<sup>[17,18]</sup>

To obtain concentrations of 250, 500, 750, 1000, 1250, 1500, and 2000 ng of lupeol per spot, various quantities of a standardized solution of lupeol were applied to the HPTLC plate. Then, the plates are scanned under UV-visible absorbance/reflectance at 530 nm wavelength to obtain densitometry measurements using the solvent system Toluene: Methanol: Formic acid (7: 2.7: 0.3 v/v/v).<sup>[19]</sup>

For analysis, a 100 g/mL methanol extract of *C. halicacabum* roots was made. The samples were filtered and then it was vacuum-dried at 45°C. The dried extracts were individually reconstituted with 1-mL of methanol and samples ranging in amount from 1 to 5 µL were spotted for analysis.<sup>[20]</sup>

#### Detection and Estimation of Lupeol

Toluene: Methanol: Formic acid (7: 2.7: 0.3 v/v/v)) was priorly saturated in a 25 mL mobile phase for 30 minutes at the temperature of the room (25°C) and 50% relative humidity in order to prepare it for lupeol. In a Camag using the chamber (20 x 10 cm), the development in a linear upward direction was completed using the CAMAG TLC Scanner "Scanner\_171010" S/N 171010 (2.01.02). The chromatogram run might have lasted up to 95 mm. The plate was quantitatively measured at 530 nm using the following settings: Micro, data resolution of 100 µm/step, scanning speed of 20 mm/sec, slit width of 4.00 × 0.30 mm, and absorption-reflection mode.<sup>[21]</sup> A 366 nm

visible spectrum was continuously emitted by a tungsten lamp, which served as the radiation source. Using pure standards, the amount of lupeol contained in methanolic extracts of *C. halicacabum* was ascertained through the external standard approach. Every task was finished three times.<sup>[22]</sup>

#### Calibration Curve and Linearity

Using a semiautomatic spotter, a standard lupeol (250–2000 ng) solution for the roots of *C. halicacabum* was placed onto precoated TLC plates. A nitrogen stream was employed to aid in the calibration procedure. After developing TLC plates, they were dried with hot air and then subjected to photometric analysis. Plotting the area of the peak against the concentration (measured in ng/spot) for each spot produced the calibration curves.<sup>[21,22]</sup>

#### Estimation of Neuroprotective potential by DPPH Antioxidant Assay

##### Preparation of inoculums

Dissolving 3.940 mg of DPPH in 100 mL of methanol produced a solution of DPPH with 100 M concentration. To keep light from getting inside, aluminium foil was wrapped around the bottle.<sup>[23]</sup> A stock solution of reference standard ascorbic acid containing 10 mg/mL was produced by mixing 100 mg of precisely weighed ascorbic acid with 10 mL methanol. By diluting the stock solution, test solutions with ascorbic acid, 50, 100, 150, 200, and 250 µg/mL concentrations were created.<sup>[23]</sup> An approximate ratio of 1:1 was used. A 0.75 mL solution of DPPH and 0.75 mL of methanol made up the control mixture. A blank of 1.5 mL methanol was added to a tube. As a reference, 0.75 mL of DPPH and 0.75 mL of ascorbic acid were combined. Plant extract and DPPH sample totaling 0.75 mL each were combined. All of these mixes were immediately stored in the shadows to protect them from light. Absorbance was taken at 517 nm wavelength after a 30-minute incubation period. Additionally, the IC<sub>50</sub> value was determined.<sup>[24]</sup>

#### Molecular Docking Study

Following the GCMS analysis, a total of 18 phytochemicals were deemed appropriate for conducting docking studies. The PubChem database, accessible at <https://pubchem.ncbi.nlm.nih.gov/>, supplied the 3-dimensional structures of these ligands in.sdf format. The Open Babel application and Auto Dock software (<https://autodock.scripps.edu/>) were used to optimize and convert these compounds to pdbqt format.<sup>[25]</sup> The auto dock was utilized to perform molecular docking and predict the binding mechanism of all phytoconstituents as inhibitors of AChE and BuChE. Auto-Dock tools assigned single bonds to flexible ligands. The enzymes BuChE (1P0I) and AChE (4PQE) were modeled in three dimensions using the RCSB protein data bank. The protein data bank crystal structure was

refined by excluding co-factors, heteroatoms, and water molecules.<sup>[26]</sup>

PyMol was used to identify the xyz coordinates after downloading the structure in.pdb format from the RCSB protein data bank and visualizing it in Biovia Discovery Studio. Optimization of pdb structures occurred after removing the water molecules, ligands, and ions. The compound was saved in pdbqt format and the coordinated ligand binding sites were set as previously identified from the active chains and bound ligands of the proteins' co-crystallized structures to create a macromolecule.<sup>[27]</sup> To replicate docking for all phytoconstituents, an active site grid was created. Sorting the output by Glide docking score revealed the best-docked compound structure. Both PyMOL and Biovia Discovery Studio were used to study and visualize these docked complexes. All phytoconstituents identified by GC-MS were predicted for ADME properties using Swiss ADME, pkCSM, and ADMETlab.<sup>[28-30]</sup>

**Table 1:** %Yield in successive solvent extraction

S. No.	Menstruum	Vibrant Hue	Appearance	%Dried extract (w/w)
1	Solvent ether	Tint Brown	Non-greasy	0.93 g
2	Toluene	Brown	Non-greasy	2.20 g
3	Methanol	Dark Brown	Non-greasy	3.2 g
4	Distilled Water	Dark Brown	Non-greasy	3.4 g

**Table 2:** Phytoconstituents identified in root extract

S. No.	Retention time (min.)	Area root extract	Height root extract
1	1.83	7.32	0.863
2	2.79	42.43	3.027
3	3.20	43.87	1.493
4	10.71	1.58	0.237

**Table 3:** %Height inhibition of AChE with physostigmine

S. No.	Retention time (min.)	Area AChE	Area AChE+ Physostigmine	Height AChE	Height AChE+ Physostigmine	%Height inhibition of AChE
1	2.49	0.37	0.21	0.135	0.096	28.889

**Table 4:** %Height inhibition of AChE with extract

S. No.	Retention time (min.)	Area extract	Area AChE + Extract	Height extract	Height AChE + extract	% Height inhibition of extract
1	1.83	7.32	6.81	0.863	0.776	10.08
2	2.79	42.43	39.82	3.027	2.755	8.98
3	3.20	43.87	35.17	1.493	1.326	11.18
4	10.71	1.58	1.04	0.237	0.178	24.89

## RESULTS

### %yield in Successive Solvent Extraction

The %yield (w/w) of the root extract with different polarity solvents of *C. halicacabum* was as given in Table 1. Methanolic root extract was used for further analysis because it identified the most active phytoconstituents in preliminary phytochemical screening with chemical tests.

### Phytochemical Screening of Methanolic Root Extract with HPLC

The HPLC screening of methanolic root extract shows four fused peaks as displayed in Table 2.

### In-vitro Acetylcholinesterase Inhibition Study by HPLC

At a retention time of 2.49 minutes, the height of AChE was inhibited by 28.88% with physostigmine as displayed in Table 3.

No acetylcholinesterase peak was observed at 2.49 minutes, indicating complete inhibition of AChE by all different phytoconstituents in root extract. From Table 4, Fig. 1, all phytoconstituents' height and area decreased, indicating their effectiveness against AChE.

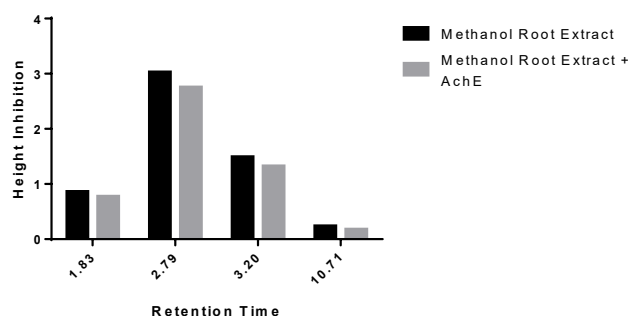


**Fig. 1:** %height inhibition of different phytoconstituents of extract with AChE



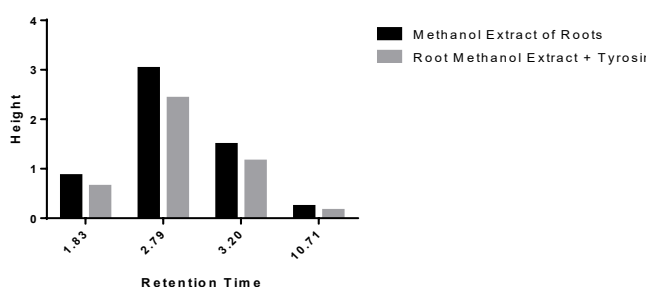


**Table 5:** %Height inhibition of tyrosinase with pregabalin

S. No.	Retention time (min.)	Area tyrosinase	Area Tyrosinase+ Pregabalin	Height tyrosinase	Height Tyrosinase+ Pregabalin	%Height inhibition of tyrosinase
1	2.97	3.55	1.29	0.447	0.227	49.218

**Table 6:** %Height inhibition of tyrosinase with extract

S. No.	Retention time (min.)	Area extract	Area Tyrosinase + Extract	Height extract	Height Tyrosinase+ extract	%Height inhibition of extract
1	1.83	7.32	6.11	0.863	0.646	25.14
2	2.79	42.43	35.59	3.027	2.426	19.85
3	3.20	43.87	29.57	1.493	1.155	22.63
4	10.71	1.58	1.02	0.237	0.160	32.48

**Fig. 2:** %height inhibition of different phytoconstituents of extract with tyrosinase**Table 7:** Rf value of crude root extract

Peak. No.	RF Value
1	0.48
2	0.51
3	0.57
4	0.67
5	0.69

**Table 8:** Rf value of isolated marker

Spot. No.	RF Value
1	0.69

### In-vitro Tyrosinase Inhibition Study by HPLC

At a retention time 2.97 minutes, the height of tyrosinase was inhibited by 49.21% with pregabalin, as displayed in Table 5.

At retention time 2.97, no tyrosinase peak was observed, indicating complete inhibition by all phytoconstituents in root extract. From Table 6, Fig. 2, all phytoconstituents' height and area decreased, indicating their effectiveness against tyrosinase.

### Isolation of Bioactive Marker Lupeol

TLC and HPTLC chromatogram of an isolated fraction of column chromatography of methanolic extract and isolated marker from *C. halicacabum* Linn. is shown in Tables 7, 8; Figs 3 (A) and (B), 4.

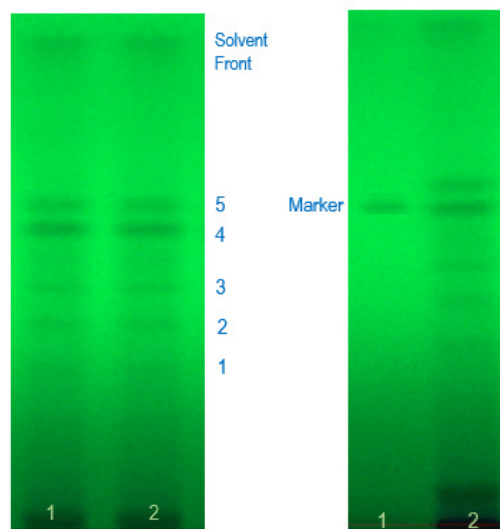
### Identification of Lupeol as a Bioactive Marker by UV Spectroscopy

The  $\lambda_{max}$  of the isolated lupeol was found 239/280 nm by UV spectroscopy.

### Estimation of Lupeol in Root Extract

#### Optimization of HPTLC chromatographic conditions

Lupeol, an antioxidant triterpenoid, was estimated from the methanolic extract. The lupeol was precisely

**Fig. 3:** (A) TLC of crude root extract and (B) TLC of isolated marker

quantified; Rf was 0.55. Lupeol and methanolic root extract chromatograms are shown. As shown in the peak, the extract and standard lupeol had similar Rf values of 0.57. Lupeol was estimated using HPTLC (Table 9, Figs 4-9).

**Table 9:** HPTLC-Lupeol profile of the methanolic extract of *C. halicacabum* Linn.

Peak	Maximum Rf	Maximum height	Maximum%	Peak area	Peak area%	Allocated substance
1	0.60	174.0	100.00	3499.4	100.00	Lupeol
2	0.58	202.9	80.16	3112.7	91.88	Lupeol
3	0.57	201.4	80.48	2736.6	90.16	Lupeol
4	0.56	209.2	100.00	2835.4	100.00	Lupeol
5	0.56	211.7	82.32	2755.0	90.40	Lupeol
6	0.56	206.0	78.70	2414.7	86.32	Lupeol
7	0.56	513.6	93.07	10829.2	98.23	Extract C.H.
8	0.57	435.0	100.00	10035.9	100.00	Extract C.H.
9	0.58	448.4	100.00	15089.5	100.00	Extract C.H.

**Table 10:** Estimation of lupeol in crude root extract

Track Vial	Sample ID	Rf	Amount (ng)	Height	X	Area	X
1	Lupeol	0.60	250	173.98		3499.37	
2	Lupeol	0.58	500	202.89		3112.66	
3	Lupeol	0.57	1000	201.39		2736.55	
4	Lupeol	0.56	1250	209.19		2835.39	
5	Lupeol	0.56	1500	211.69		2755.03	
6	Lupeol	0.56	2000	206.05		2414.69	
7	Extract C.H.	0.56		513.6	>2.200 µg	10829.2	>6.400 µg
8	Extract C.H.	0.57		435.0	>2.200 µg	10035.9	>6.400 µg
9	Extract C.H.	0.58		448.4	>2.200 µg	15089.5	>6.400 µg

### HPTLC Spectra of Karnasphota Root Extract and Standard Lupeol

#### Calibration curve and linearity

Table 10 and Fig. 10 presented the correlation curves and regression equations for lupeol in the roots of *C. halicacabum* L. The regression via height was represented by the equation  $Y = 184.3 + 0.01528 * X$ , with a correlation coefficient of  $r = 0.98755$  and a standard deviation of 0.70. The regression via area was represented by the equation  $Y = 3478 + -0.5405 * X$ , with a correlation coefficient of  $r = 0.98917$  and a standard deviation of 0.71.

#### DPPH Antioxidant Assay

The methanolic extract made from *C. halicacabum* roots has potent antioxidant qualities, as shown by the in vitro DPPH free radical scavenging experiment. As a positive control, ascorbic acid was utilized; its inhibitory concentration 50% value was 88.22 µg (Table 11, Fig. 11). As indicated in Table 12, Fig. 12, the  $IC_{50}$  values for the capacity to scavenge DPPH free radicals in roots were found to be 89.08 µg, which is comparable to the efficacy of ascorbic acid.

#### In-silico screening of phytoconstituents against AChE

GCMS analysis of root extract identified optimal phytoconstituents and predicted their interactions with

**Table 11:**  $IC_{50}$  of ascorbic acid

Ascorbic acid (µg/mL)	%Scavenging activity (A0-A1 * 100)/A0	SD with respect to %Inhibition	$IC_{50}$
0 (Blank)	0.00	0.421	88.22 µg
50	3.373*	1.191	
100	21.187***	0.646	
150	57.287****	1.708	
200	69.433****	1.390	
250	83.603****	2.138	

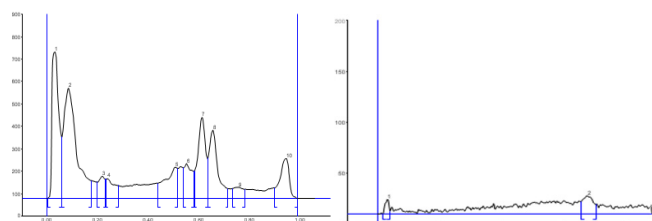
**Table 12:**  $IC_{50}$  of root extract

MeOH extract (µg/mL)	%Scavenging activity (A0-A1 * 100)/A0	SD with respect to %Inhibition	$IC_{50}$
0 (Blank)	0.00	1.022	89.08 µg
50	21.881***	0.155	
100	33.742****	0.687	
150	48.261****	0.981	
200	62.167****	1.525	
250	76.073****	1.483	



**Table 13:** Docking energies of compounds with AChE and BuChE

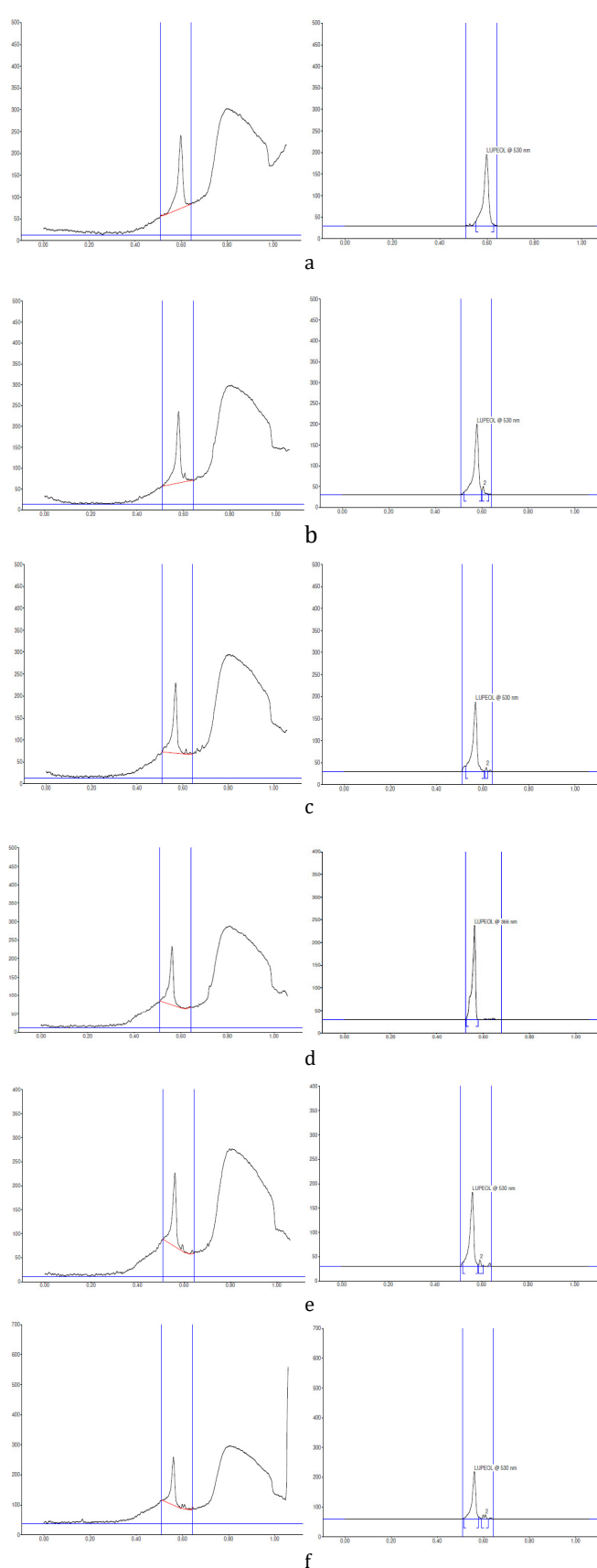
S. No.	Name of ligand	Affinity Score (Kcal/ mol) AChE
1	Phthalic acid, di(2-propylpentyl) ester	-7.7
2	1,2-Benzenedicarboxylic acid, bis(2-ethylhexyl) ester	-7.8
3	1,2-Benzenedicarboxylic acid, bis(2-methylpropyl) ester	-8.1
4	3,7,11,15-Tetramethyl-2-hexadecen-1-ol	-7.6
5	Dibutyl phthalate	-7.5
6	Hexadecanoic acid, methyl ester	-5.9
7	1,2-Benzenedicarboxylic acid, bis(2-ethylhexyl) ester	-7.8
8	Cholesta-5,22-dien-3-ol, (3.β.)	-10.2
9	Ergosta-5,22-dien-3-ol, (3.β.,22E)	-10.5
10	24-Noroleana-3,12-diene	-8.7
11	Olean-12-en-3-ol, acetate, (3.β.)	-9.6
12	Lup-20(29)-en-3-ol, acetate, (3.β.)	-8.2
13	Lup-20(29)-en-3-one	-8.4
14	Urs-12-en-3-ol, acetate, (3.β.)	-8.4
15	Acetic acid, 4,4a,6b,8a,11,11,12b,14a-octamethyl-3-oxodocosahydricen-2-yl ester	-10.1
16	Gamma sitosterol	-9.5
17	Stigmasterol	-9.6
18	α-Amyrin	-10.2
19	Donepezil	-8.4

**Fig. 4:** Comparative HPTLC chromatogram of crude root extract and isolated marker

AChE's AD targets (PDB ID: 4PQE). Supplemental Table 13 shows the ligand-receptor binding energy of each tentatively identified phytoconstituent. Potential lead compounds were chosen from molecules with the highest receptor binding affinity to show 2D and 3D interactions (Fig. 13).

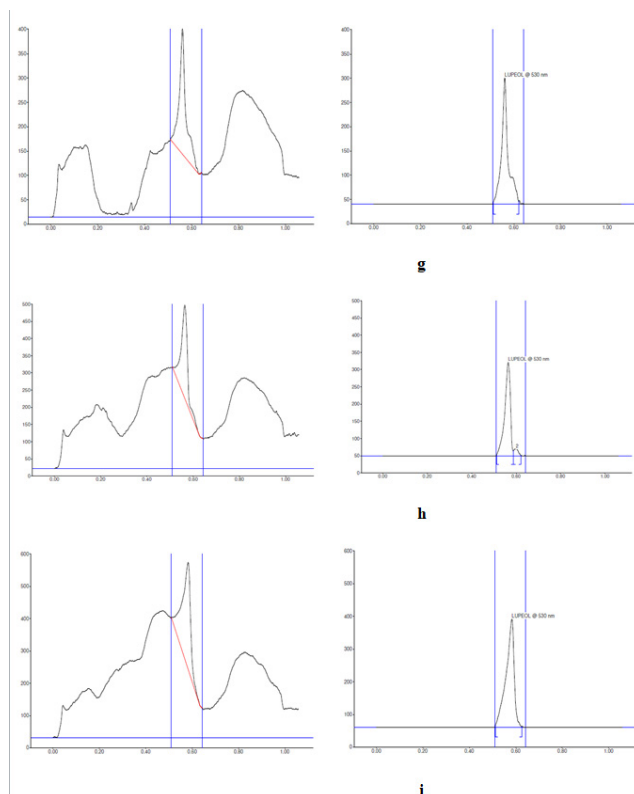
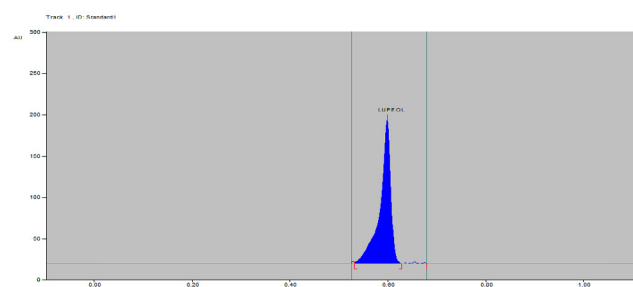
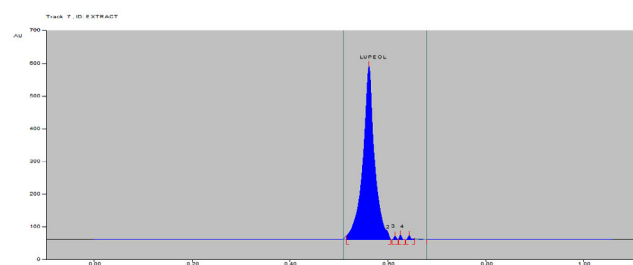
#### Predicted drug likeliness profile

The drug-likeness profile for all phytoconstituents of *C. halicacabum* L. in Table 14 assesses the likelihood

**Fig. 5:** The Lupeol standard spectrum of various concentrations ranging from a to f

**Table 14:** Drug likeliness profile

Name of compound	Molecular Weight (gm/mol)	H Bond Donor	H Bond Acceptor	MLogP	Bioavailability Score	Synthetic Accessibility	Lipinski Likeliness	Lipinski Violation
Phthalic acid, di(2-propylpentyl) ester	390.56	0	4	5.24	0.55	3.39	Yes	1
1,2-Benzenedicarboxylic acid, bis(2-ethylhexyl) ester	390.56	0	4	5.24	0.55	4.12	Yes	1
1,2-Benzenedicarboxylic acid, bis(2-methylpropyl) ester	250.29	0	4	2.68	0.55	2.15	Yes	0
2-Hexadecen-1-ol, 3,7,11,15-tetramethyl-, acetate, [R-[R*,R*-(E)]]	354.61	0	2	7.57	0.55	4.73	Yes	1
Dibutyl phthalate	278.34	0	4	3.43	0.55	2.41	Yes	0
Hexadecanoic acid, methyl ester	270.45	0	2	4.44	0.55	2.53	Yes	1
1,2-Benzenedicarboxylic acid, bis(2-ethylhexyl) ester	390.56	0	4	5.24	0.55	4.12	Yes	1
Cholesta-5,22-dien-3-ol, (3.beta.)	384.64	1	1	6.23	0.55	5.90	Yes	1
Ergosta-5,22-dien-3-ol, (3.beta.,22E)	398.66	1	1	6.43	0.55	6.09	Yes	1
24-Noroleana-3,12-diene	410.72	0	0	7.89	0.55	6.22	Yes	1
Olean-12-en-3-ol, acetate, (3.beta.)	468.75	0	2	7.08	0.55	5.98	Yes	1
Lup-20(29)-en-3-ol, acetate, (3.beta.)	468.75	0	2	7.08	0.55	5.66	Yes	1
Lup-20(29)-en-3-one	424.70	0	1	6.82	0.55	5.38	Yes	1
Urs-12-en-3-ol, acetate, (3.beta.)	468.75	0	2	7.08	0.55	6.11	Yes	1
Acetic acid, 4,4a,6b,8a,11,11,12b,14a-octamethyl-3-oxodocosahydricen-2-yl ester	484.75	0	3	6.20	0.55	5.68	Yes	1
Gamma Sitosterol	446.79	1	1	7.12	0.55	6.71	Yes	1
Stigmasterol	412	1	1	6.62	0.55	6.21	Yes	1
$\alpha$ -Amyrin	442.76	1	1	7.12	0.55	6.37	Yes	1

**Fig. 6:** Spectra of methanolic root extract of *C. halicacabum* Linn. ranging from G to I**Fig. 7:** Standard lupeol profile by HPTLC chromatogram**Fig. 8:** HPTLC chromatogram of lupeol in *C. halicacabum* L. methanolic root extract

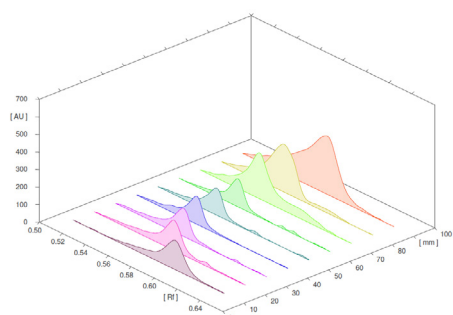
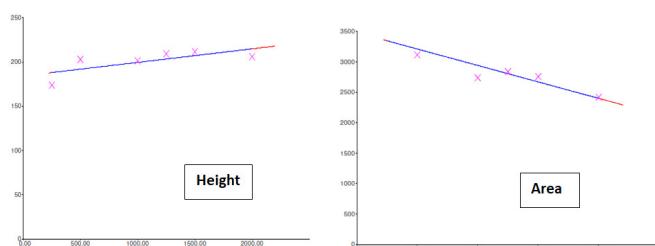
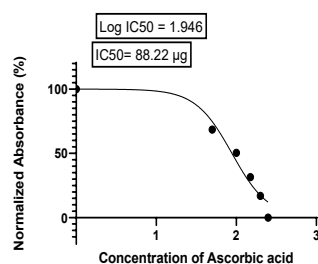
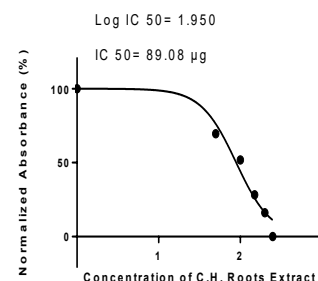
that a compound will have the pharmacological and physicochemical properties needed to develop a safe and effective drug.





**Table 15:** ADMET profile

Name of Compound	Water solubility (log mol/L)	Caco2 permeability (log Papp in 10 <sup>-6</sup> cm/s)	Intestinal absorption (human) (% Absorbed)	VDss (human) (log L/kg)	BBB permeability (log BB)	CYP3A4 substrate	Total Clearance (log ml/min/kg)	Max. tolerated dose (human) (log mg/kg/day)
Phthalic acid, di(2-propylpentyl) ester	-6.433	1.41	91.988	0.326	-0.228	Yes	1.88	1.383
1,2-Benzenedicarboxylic acid, bis(2-ethylhexyl) ester	-6.722	1.404	91.552	0.405	-0.161	Yes	1.833	1.371
1,2-Benzenedicarboxylic acid, bis(2-methylpropyl) ester	-5.27	1.521	94.093	-0.02	-0.017	Yes	0.776	1.442
2-Hexadecen-1-ol, 3,7,11,15-tetramethyl-, acetate, [R-[R*,R*-(E)]]	-7.923	-7.923	92.376	0.389	0.75	Yes	1.562	0.16
Dibutyl phthalate	-4.169	1.622	95.044	-0.007	-0.054	Yes	0.93	1.536
Hexadecanoic acid, methyl ester	-6.927	1.6	92.335	0.334	0.749	Yes	1.861	0.178
1,2-Benzenedicarboxylic acid, bis(2-ethylhexyl) ester	-6.47	1.408	92.45	0.36	-0.175	Yes	1.898	1.393
Cholesta-5,22-dien-3-ol, (3.β.)	-6.998	1.243	95.609	0.316	0.765	Yes	0.581	-0.352
Ergosta-5,22-dien-3-ol, (3.β.,22E)	-7.156	1.252	96.423	0.368	0.775	Yes	0.57	-0.195
24-Noroleana-3,12-diene	-7.631	1.302	96.984	0.746	0.853	Yes	0.057	0.247
Olean-12-en-3-ol, acetate, (3.β.)	-7.038	1.285	98.202	0.272	0.655	Yes	-0.134	0.378
Lup-20(29)-en-3-ol, acetate, (3.β.)	-6.412	1.277	100	-0.122	0.711	Yes	0.064	0.342
Lup-20(29)-en-3-one	-6.346	1.374	100	0.006	0.774	Yes	0.102	0.346
Urs-12-en-3-ol, acetate, (3.β.)	-7.046	1.27	100	0.362	0.618	Yes	0.025	0.007
Acetic acid, 4,4a,6b,8a,11,11,12b,14a-octamethyl-3-oxodocosahydricipen-2-yl ester	-6.238	1.314	100	-0.222	-0.618	Yes	-0.147	0.346
Beta Sitosterol	-7.233	1.259	94.086	0.133	0.78	Yes	0.737	-0.271
Stigmasterol	-7.137	1.243	96.154	0.259	0.786	Yes	0.618	-0.264
α-Amyrin	-6.687	1.359	96.306		0.67	Yes	0.105	-0.078

**Fig. 9 :**3D HPTLC chromatogram of lupeol standard and extract**Fig. 10:** Calibration curve and linearity profile by height and area**Fig. 11:** Graphical presentation of IC<sub>50</sub> of ascorbic acid**Fig. 12:** Graphical presentation of IC<sub>50</sub> of root extract

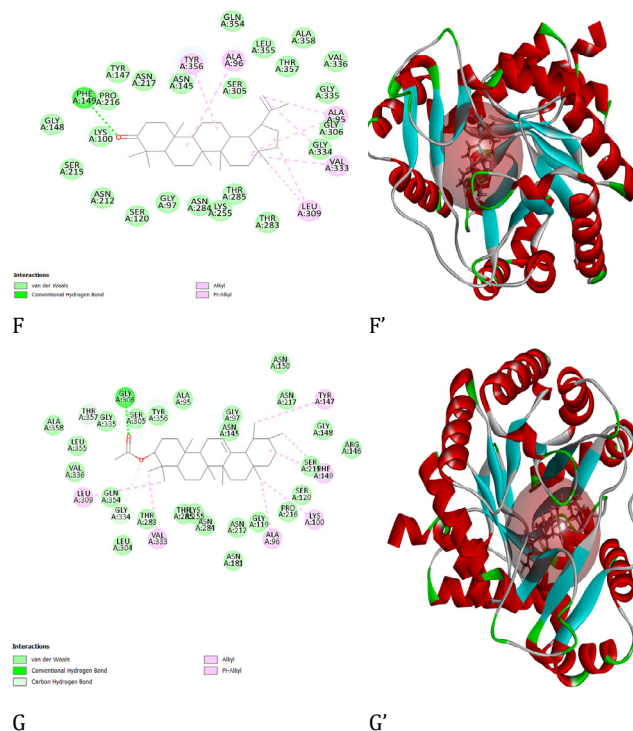
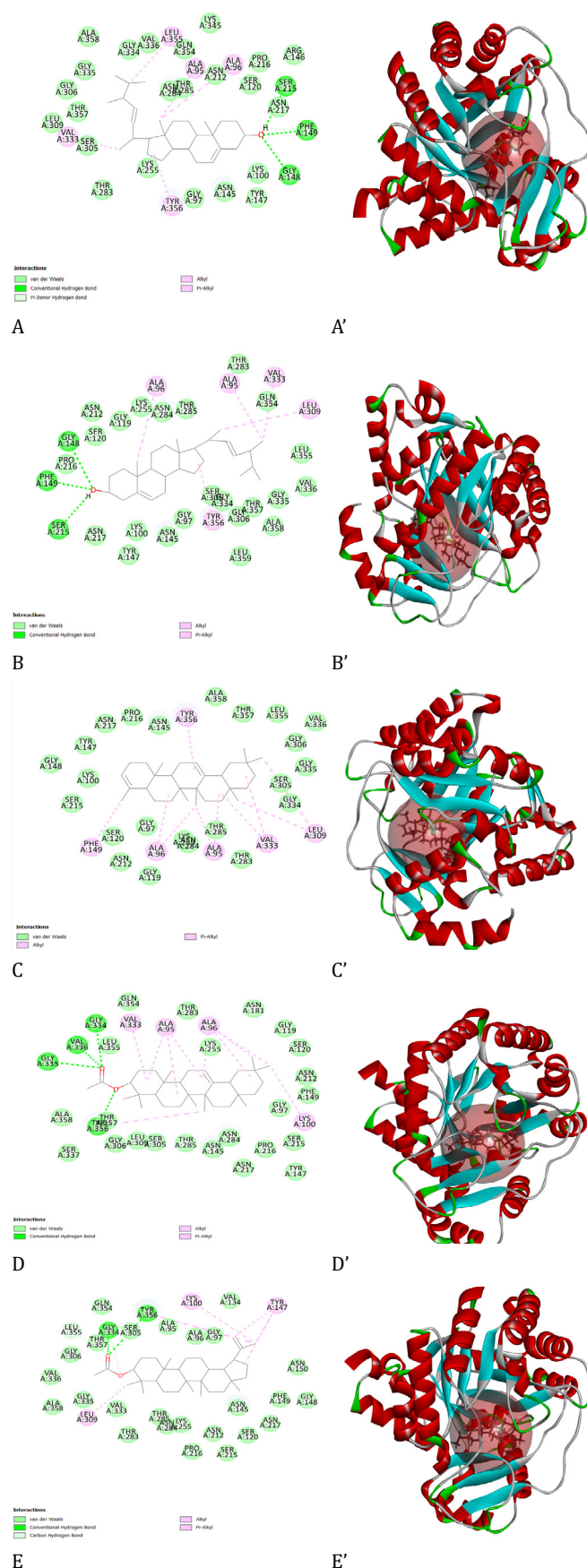


**Fig. 13:** Binding Interaction of 4PQE with phytoconstituents from *C. halicacabum* L. (A) 2D interaction of Cholesta-5,22-dien-3-ol, (3.β.), (A') 3D interaction of Cholesta-5,22-dien-3-ol, (3.β.), (B) 2D interaction of Ergosta-5,22-dien-3-ol, (3.β.,22E), (B') 3D interaction of Ergosta-5,22-dien-3-ol, (3.β.,22E), (C) 2D interaction of 24-Noroleana-3,12-diene, (3.β.), (C') 3D interaction of 24-Noroleana-3,12-diene, (D) 2D interaction of Olean-12-en-3-ol, acetate, (3.β.), (D') 3D interaction of Olean-12-en-3-ol, acetate, (3.β.), (E) 2D interaction of Lup-20(29)-en-3-ol, acetate, (3.β.), (E') 3D interaction of Lup-20(29)-en-3-ol, acetate, (3.β.), (F) 2D interaction of Lup-20(29)-en-3-one, (F') 3D interaction of Lup-20(29)-en-3-one, (G) 2D interaction of Urs-12-en-3-ol, acetate, (3.β.), (G') 3D interaction of Urs-12-en-3-ol, acetate, (3.β.).

### Predicted ADMET Properties

A docking study was used to predict ADMET for the extract's optimal ligands. Computing tools and algorithms used in docking studies predict ADMET properties based on candidate compounds' molecular structures. Integrating ADMET predictions with docking results prioritizes compounds with good pharmacokinetic and safety profiles for experimental validation, speeding up drug discovery. Table 15 shows intestinal absorption, BBB penetration, carcinogenicity, and acute oral toxicity.

### CONCLUSION

The methanolic root extract of *C. halicacabum* L. contains many biologically active phytoconstituents that inhibit acetylcholinesterase and tyrosinase enzymes, suggesting therapeutic benefits. *C. halicacabum* L. roots exhibit strong neuroprotective effects, with the  $IC_{50}$  value of 89.08  $\mu\text{g/mL}$  in the DPPH antioxidant assay. This value matches ascorbic acid, demonstrating the extract's antioxidant properties.



HPLC analysis showed that the extract's phytoconstituents are quite potent compared to standards. The extract contains triterpene lupeol, a bioactive marker that is identified anti-inflammatory, antioxidant, and neuroprotective agent, contributing to the extract's neuroprotective potential. The docking analysis of phytoconstituents identified by GC-MS analysis from karnasphota root extract demonstrates favorable interactions with the culprit enzyme protein 4PQE (Crystal structure of human acetylcholinesterase) as described here. These findings suggest the plant's potential use in pharmaceutical and nutraceutical applications aimed at treating conditions involving oxidative stress and neurodegeneration.

## REFERENCES

- Mannangatti P, Naidu KN. Indian herbs for the treatment of neurodegenerative disease. In: *Advances in Neurobiology*. Cham: Springer International Publishing; 2016. p. 323–36.
- Rao K, Hegde ML, Anitha S. Amyloid  $\beta$  and neuromelanin - toxic or protective molecules? The cellular context makes the difference. *Prog Neurobiol*. 2006;78:364–73.
- Ilies M, Banciu MD, Ilies MA, Scozzafava A, Caproiu MT, Supuran CT. Carbonic anhydrase activators: design of high affinity isozymes I, II, and IV activators, incorporating tri-/tetrasubstituted-pyridinium-azole moieties. *J Med Chem [Internet]*. 2002;45(2):504–10. Available from: <http://dx.doi.org/10.1021/jm011031n>
- Temperini C, Scozzafava A, Supuran CT. Carbonic anhydrase activation and the drug design. *Curr Pharm Des [Internet]*. 2008;14(7):708–15. Available from: <http://dx.doi.org/10.2174/138161208783877857>
- Kartika B, Muralidharan P, Rahman H. Herbal treatment of Parkinsonism: a review. *International Journal of Pharmaceutical Sciences Review and Research*. 2010;5(3):185–91.
- Kumar E, Mastan SK, Sreekanth N, Chaitanya G, Reddy GA, Raghunandan N. Anti-Arthritic Property of the Ethanolic Leaf Extract of *Cardiospermum halicacabum* Linn. *Biomedical and Pharmacology Journal*. 2015;1(2):395–400.
- Asha VV, Pushpangadan P. Antipyretic activity of *Cardiospermum halicacabum*. *Indian J Exp Biol*. 1999;37(4):411–4.
- Dowlath M, Karuppannan SK, Darul R, Mohamed K, Subramanian S, Arunachalam KD. Effect of Solvents on Phytochemical Composition and Antioxidant Activity of *Cardiospermum halicacabum* (L.) Extracts. *Pharmacogn J*. 2020;12(6):1241–51.
- Topiya HR, Pandya DJ. Karnasphota: A neuroprotective herb from the treasure of Ayurveda. *Curr Tradit Med [Internet]*. 2023;10. Available from: <http://dx.doi.org/10.2174/2215083810666230905152757>
- Li Q, Mo J, Xiong B, Liao Q, Chen Y, Wang Y, et al. Discovery of resorcinol-based polycyclic structures as tyrosinase inhibitors for treatment of Parkinson's disease. *ACS Chem Neurosci [Internet]*. 2022;13(1):81–96. Available from: <http://dx.doi.org/10.1021/acscchemneuro.1c00560>.
- Kumaran A, Karunakaran J. Antioxidant Activities of the Methanol Extract of *Cardiospermum halicacabum*. *Pharmaceutical biology*. 2006;44:146–51
- World Health Organization. General guidelines for methodologies on research and evaluation of traditional medicine. World Health Organization. 2000.
- Analysis of questionnaire on traditional medicine. Geneva World Health Organization. 1992.
- Kanani SH, Pandya DJ. The phytochemical screening, total cucurbitacin content, and in vitro anti-breast cancer activity of *Leucopaxillus gentianeus* mushroom. *Future Journal of Pharmaceutical Sciences*. 2023;9(1).
- Abdullahi SM, Musa AM, Abdullahi MI, Sule MI, Sani YM. Isolation of Lupeol from the Stem-bark of *Lonchocarpus sericeus* (Papilionaceae). *Scholars Acad J Biosci*. 2013;1(1):18–9.
- Sánchez-Burgos JA, Ramírez-Mares MV, Gallegos-Infante JA, González-Laredo RF, Moreno-Jiménez MR, Cháirez-Ramírez MH, et al. Isolation of lupeol from white oak leaves and its anti-inflammatory activity. *Industrial crops and products*. 2015;77:827–32.
- Suthar AC, Banavaliker MM, Biyani MK, Indira P, Sudarsan K, Mohan V. High-performance thin layer chromatography method for quantitative estimation of lupeol in *Crataeva nurvala*. *Indian Drugs*. 2001;38(9):474–8.
- Badami S, Gupta MK, Ramaswamy S, Rai SR, Nanjaian M, Bendell DJ, et al. Determination of betulin in *Grewia titiaefolia* by HPTLC. *J Separ Sci*. 2004;27:129–31.
- Purnima D, Hamrapurkar PK. HPTLC determination of stigmasterol and tocopherol acetate in *Leptadenia reticulata* and its formulation. *J Plan Chromatogr*. 2007;20(3):183–7.
- Guideline IH. Validation of analytical procedures: text and methodology. Q2 (R1). 1920.
- Ravindra CS, Sanjay BK, Kalaichelvan VK. Phytochemical profile studies on the steroids of methanolic leaf extract of medicinally important plant *Holoptelea integrifolia* (Roxb.) planch using high-performance thin layer chromatography. *Asian J Pharm Clin Res*. 2014;7.
- Lavanya MS, Gnanamani A, Ilavarasan R. Physico-chemical, phytochemical and high-performance thin layer chromatography analysis of the whole plant of *Orthosiphon thymiflorus* (Roth.) sleesen. *Asian J Pharm Clin Res*. 2015;8.
- Braca A, Tommasi ND, Bari LD, Pizzi C, Politi M, Morelli I. Antioxidant principles from *Bauhinia terapotensis*. *J Nat Prod*. 2001;64:892–5.
- Shimada K, Fujikawa K, Yahara K, Nakamura T. Antioxidative properties of xanthan on the autoxidation of soybean oil in cyclodextrin emulsion. *J Agric Food Chem [Internet]*. 1992;40(6):945–8. Available from: <http://dx.doi.org/10.1021/jf00018a005>
- Bharathi A, Roopan SM, Vasavi CS, Munusami P, Gayathri GA, Gayathri M. In silico molecular docking and in vitro antidiabetic studies of dihydropyrimido[4,5-a]acridin-2-amines. *Biomed Res Int [Internet]*. 2014;2014:971569. Available from: <http://dx.doi.org/10.1155/2014/971569>
- Kanani SH, Ibrahim FM, Pandya DJ. Molecular docking of phytochemicals targeting ER, PR, and HER2 receptors as therapeutic sites for breast cancer: An in silico study. In: *Nanotechnology and In Silico Tools*. Elsevier; 2024. p. 357–76.
- Vegad UG, Gajjar ND, Nagar PR, Chauhan SP, Pandya DJ, Dhameliya TM. In silico screening, ADMET analysis and MD simulations of phytochemicals of *Onosma bracteata* Wall. as SARS CoV-2 inhibitors. *3 Biotech [Internet]*. 2023;13(7):221. Available from: <http://dx.doi.org/10.1007/s13205-023-03635-7>
- Kryger G, Silman I, Sussman JL. Structure of acetylcholinesterase complexed with E2020 (Aricept®): implications for the design of new anti-Alzheimer drugs. *Structure*. 1999;7(3):297–307.
- Taha M, Ismail NH, Imran S, Selvaraj M, Rahim F. Synthesis of novel inhibitors of  $\beta$ -glucuronidase based on the benzothiazole skeleton and their molecular docking studies. *RSC Adv [Internet]*. 2016;6(4):3003–12. Available from: <http://dx.doi.org/10.1039/c5ra23072a>
- Mathura VS, Paris D, Ait-Ghezala G, Quadros A, Patel NS, Kolippakkam DN, et al. Model of Alzheimer's disease amyloid-beta peptide based on a RNA binding protein. *Biochem Biophys Res Commun [Internet]*. 2005;332(2):585–92. Available from: <http://dx.doi.org/10.1016/j.bbrc.2005.04.164>

**HOW TO CITE THIS ARTICLE:** Topiya HR, Pandya DJ. Phytochemical Screening, Isolation and Estimation of Bioactive lupeol, *In-vitro* and *In-silico* Neuroprotective Effect of Phytoconstituents from Karnasphota: *Cardiospermum halicacabum* Linn. Roots. *Int. J. Pharm. Sci. Drug Res*. 2024;16(5):793-803. DOI: 10.25004/IJPSDR.2024.160507